



Non-Trivial Transport Interface in a Hybrid Topological Material With Hexagonal Lattice Arrangement

Lianlian Du, Yahong Liu*, Meize Li, Huiling Ren, Kun Song* and Xiaopeng Zhao

School of Physical Science and Technology, Northwestern Polytechnical University, Xi'an, China

In this paper, a hybrid topological material with hexagonal lattice arrangement is proposed, consisting of six metal cylindrical resonators and a dielectric slab. As a unit cell, the six metal cylindrical resonators satisfying the C_6 symmetry are selected, and the cylindrical resonators are inserted in the dielectric slab. It is demonstrated that a double Dirac cone is created at the Γ point in the proposed topological material. Since the topological effects of the proposed system can be invoked merely by varying the geometric parameters of the unit cell, two band gaps with different topological characteristics can be easily achieved. It is further demonstrated that the topologically protected edge states can be obtained by connecting the two types of lattices with different topological characteristics. Finally, we implement a sharp bend waveguide by using these two types of the topological lattices. It is demonstrated that electromagnetic waves can propagate robustly along the sharp bend interface.

Keywords: topological material, band gap, topological characteristics, edge states, non-trivial transport, interface

OPEN ACCESS

Edited by:

Xingzhan Wei,
Chongqing Institute of Green and
Intelligent Technology (CAS), China

Reviewed by:

Hongchao Liu,
University of Macau, China
Jinhui Shi,
Harbin Engineering University, China

*Correspondence:

Yahong Liu
yhliu@nwpu.edu.cn
Kun Song
songkun@nwpu.edu.cn

Specialty section:

This article was submitted to
Optics and Photonics,
a section of the journal
Frontiers in Physics

Received: 17 August 2020

Accepted: 29 September 2020

Published: 06 November 2020

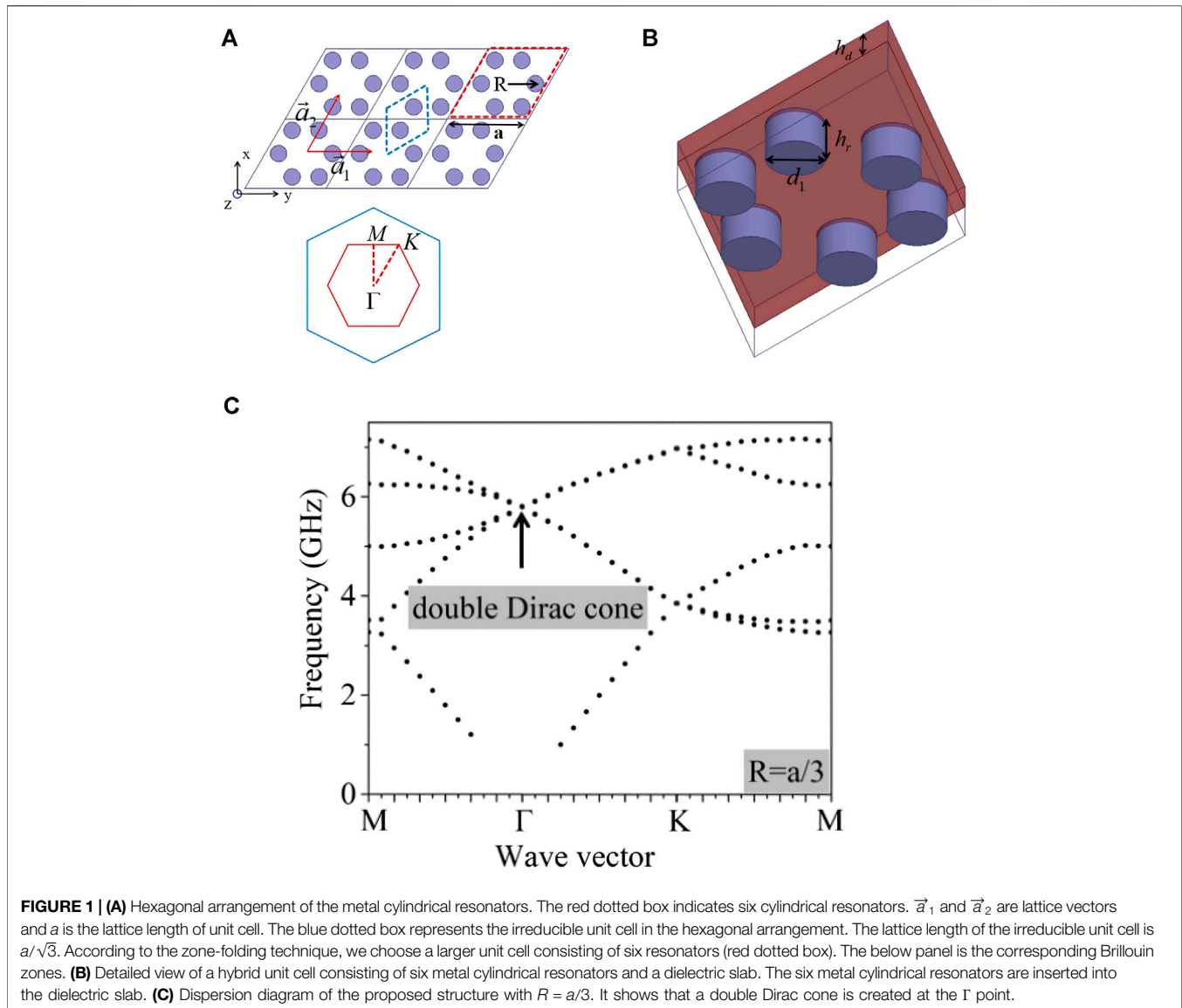
Citation:

Du L, Liu Y, Li M, Ren H, Song K and
Zhao X (2020) Non-Trivial Transport
Interface in a Hybrid Topological
Material With Hexagonal
Lattice Arrangement.
Front. Phys. 8:595621.
doi: 10.3389/fphy.2020.595621

INTRODUCTION

Topological insulator is a kind of new phase of matter state about electron conductivity proposed by condensed-matter physicists. It soon becomes a hot topic in condensed matter physics and quantum materials [1, 2]. Topological insulator is realized firstly by electrons. The interior of a topological insulator is insulated, but there is always a conductive edge state on its boundary or surface. The edge state of the topological insulators is stable, and the motion direction of conducting electrons with different spins is opposite. Therefore, the transmission can be controlled by the spin of the electron, rather than transmitted by electric charge as traditional materials, and this process does not involve dissipation.

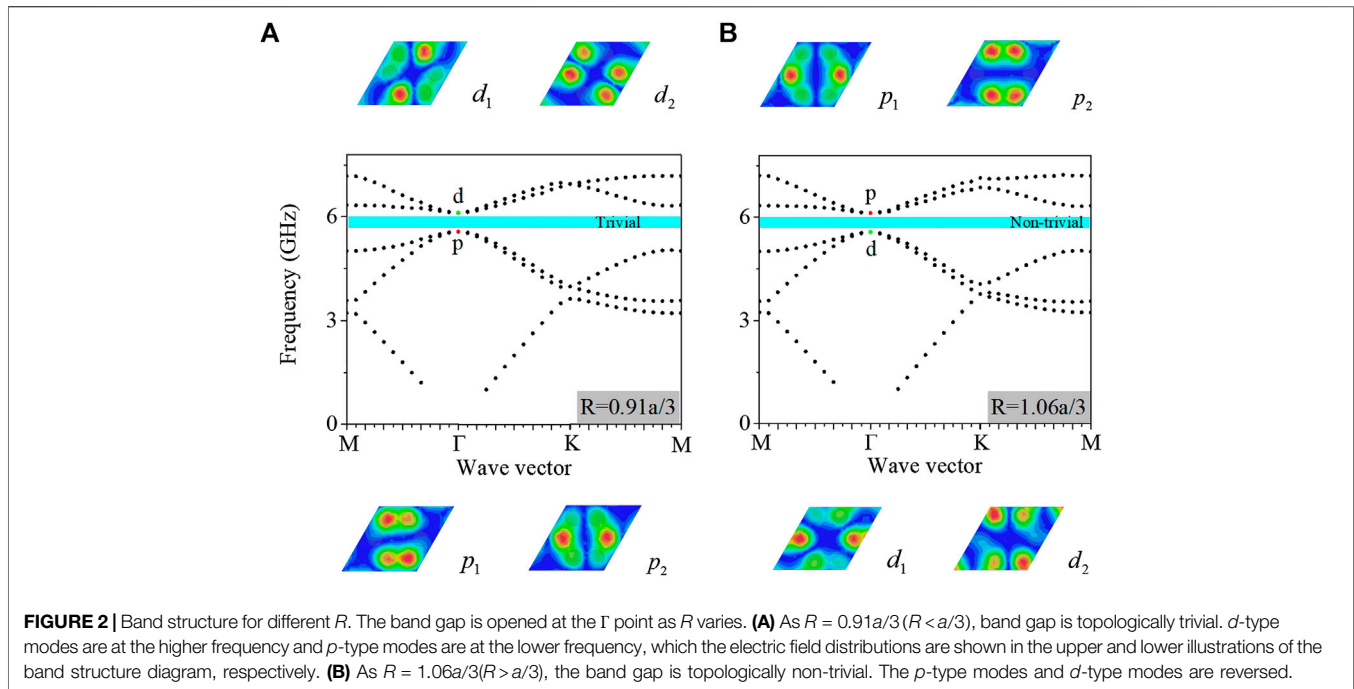
Recently, topological insulators have been extended to further areas of photonics [3–7], mechanics [8–13] and acoustics [14–21]. Topological insulators are different from conventional insulators in that the spin-orbit coupling effect of topological insulators is relatively significant. Based on the spin-orbit coupling effect, some researchers proposed a new topological crystalline insulators state [22–27]. For instance, Yang et al. proposed a chiral hyperbolic photonic metamaterial with broken inversion symmetry [26]. Ma et al. proposed a photonic topological insulator with complete topological band gap, which can emulate spin-orbit interaction through bianisotropy [27]. The quantum spin Hall effect is one of the most unique effects of topological insulators [28–31]. Wu et al. presented quantum spin Hall effect in photonic crystals [30]. Yang et al. investigated the pseudo-spin edge states for flexural waves in a honeycomb perforated phononic plate, which behaves an elastic analogue of the quantum spin Hall effect [31].



Besides the quantum spin Hall effect, topological edge state has also set off a research boom. Tzuhsuan et al. proposed a photonic structure consisting of metal rods arranged as a hexagonal array lattice, and demonstrated scattering-free edge states [32]. Huo et al. proposed two-dimensional solid phononic crystal structures, which simultaneously supported the topologically protected edge states for out-of-plane and in-plane bulk elastic waves [33]. Besides metal-based topological materials, dielectric-based topological materials have also been investigated in recent years. Xu et al. proposed a triangle photonic crystal by using core-shell dielectric materials, and demonstrated a helical edge states [34]. Xie et al. proposed a second-order topological insulator in dielectric photonic crystals and visualized one-dimensional topological edge states [35]. The topologically protected edge state has excellent characteristics of robustness, back-scattering suppression and defect immunity [36–40], which have potential applications for manufacturing new computer

chips and other components in the future. In addition, topological insulators can also have been widely applied to the fields of transport in photonic crystals [41], phonon crystals [42] and even circuits composed of classical electronic components [43].

Different from the dielectric-based topological materials or metal-based topological materials presented in the previous references, in this paper, we propose a hybrid topological model consisting of metal and dielectric materials. It provides a new method to realize the topological edge state. The hybrid topological material consists of six metal cylindrical resonators and a dielectric slab. The six cylindrical resonators are inserted into the dielectric slab. The zone-folding technique [44] (using a larger unit cell instead of an irreducible one in a hexagonal crystal lattice) is applied to this present system, so that the double Dirac cone can be generated easily at the Γ point. We demonstrate that the topologically non-trivial and trivial band gaps can be opened



near the double Dirac cone by varying the parameter R . Therefore, the topologically protected edge states can be realized easily by combining two types of lattices with different topological characteristics in the proposed system. Finally, we construct a directional sharp bend waveguide, which shows the robustness propagation of electromagnetic waves is observed in the sharp bend waveguide interface.

THEORETICAL MODEL AND BAND STRUCTURE OF THE HYBRID TOPOLOGICAL MATERIAL

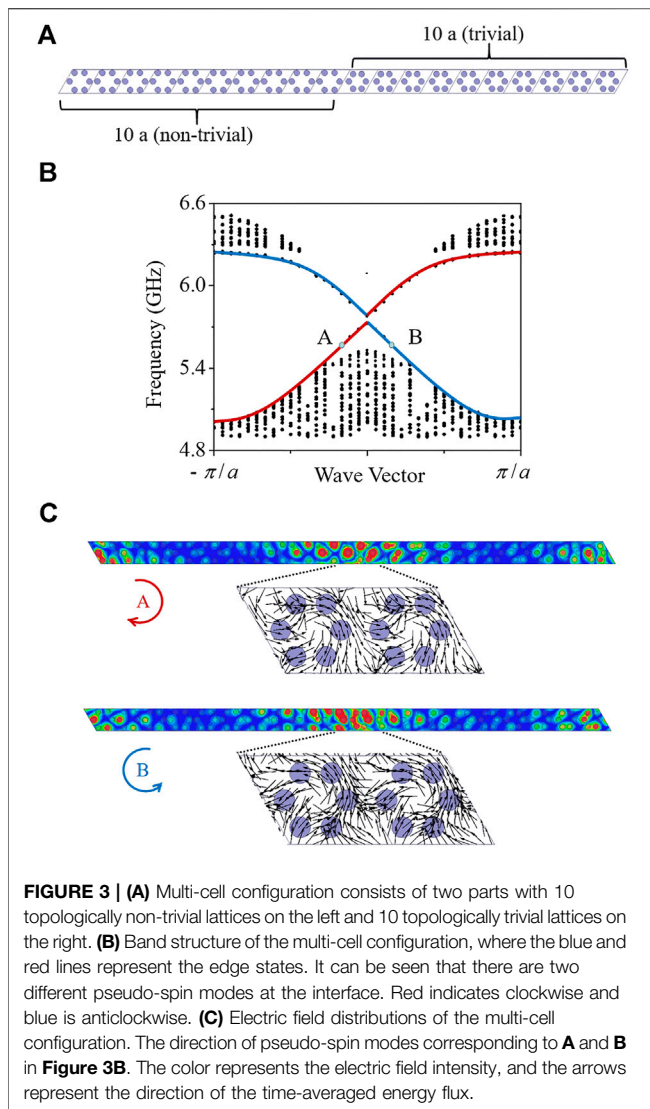
A hexagonal arrangement of the metal cylindrical resonators is shown in **Figure 1A**. The six cylindrical resonators are inserted into a dielectric slab as presented in **Figure 1B**. We choose rhombus-shaped unit cell, where the relevant parameters are shown as follows: the lattice length of unit cell is a , and the distance between the center of each resonator to the center of rhombus-shaped unit cell is R . Each rhombus-shaped unit cell includes six cylindrical resonators in a hexagonal arrangement, showing the C_6 symmetry.

Numerical simulations are performed by using a commercial simulation software High Frequency Structure Simulation Software (HFSS) based on three-dimensional finite element numerical analysis. The metal cylindrical resonators are defined as PEC, and the dielectric slab is Teflon with the relative permittivity of 2.1 and the thickness of $h_d = 2.5\text{mm}$. The size of the unit cell is $a = 17\sqrt{3}\text{mm}$, and $R = a/3$. The diameter and the height of the cylindrical resonator are both 6 mm (i.e., $d_1 = h_r = 6\text{mm}$). The periodic boundary conditions are introduced in the direction of the two lattice vectors. Based on the zone-folding technique, as shown in **Figure 1A**, we select a

unit cell composed of six resonators instead of two resonators. **Figure 1C** presents the band structure, which shows a double Dirac cone is created at the Γ point ($f_d = 5.55\text{GHz}$).

As shown in **Figure 2**, it is demonstrated that the band structure can be changed by varying the parameters R . The band inversion can be realized by different values of R . When R is shrunk (**Figure 2A**) or expanded (**Figure 2B**), it can be seen that a complete band gap appears, and simultaneously, the double Dirac cone becomes two double-degenerate modes. The emergence of band gap is due to the change in translational periodicity of the resonators. Keeping the C_6 symmetry, these double-degenerate modes are located above and below the Dirac frequency, respectively. Analogy to electronic orbital shapes, as $R = 0.91a/3$, the lower frequency modes are p -type (p_1 and p_2 as shown in the bottom of **Figure 2A**), and the higher frequency modes are d -type (d_1 and d_2 , upper in **Figure 2A**). However, as $R = 1.06a/3$, the topological characteristic of the band gap is completely different from the case of $R = 0.91a/3$. As shown in **Figure 2B**, the degenerate modes are flipped, p -type modes are at the higher frequency and d -type are at the lower frequency. That is to say, band inversion is realized as R varies.

We use the method proposed by Takahiro Fukui et al. [45] to calculate the spin Chern number of the proposed topological material. As $R = 0.91a/3$, the spin Chern number is zero, indicating topologically trivial. In contrast, as $R = 1.06a/3$, the bands have non-zero spin Chern number, which shows the topologically non-trivial. The change of spin Chern number indicates the topological phase transition. Combined **Figure 1C** and **Figure 2**, it can be seen that there is a band gap near the Dirac frequency. As R is shrunk, the double Dirac cone is opened and a complete band gap occurs. In contrast, as R is expanded, the double Dirac cone can also be opened and a band inversion occurs with the topological phase transition. These results



indicate the proposed topological material can possess the characteristics from topologically trivial to topologically non-trivial.

TOPOLOGICAL EDGE STATES

In this section, we combine topologically non-trivial ($R = 1.06a/3$) and topologically trivial ($R = 0.91a/3$) lattices to form multi-cell configurations, and study wave guiding characteristics. As shown in Figure 3A, the multi-cell configuration consists of two parts, with 10 topologically non-trivial lattices on the left and 10 topologically trivial lattices on the right. In the simulations, the periodic boundary conditions are introduced in the direction of the two lattice vectors. The band structure of the multi-cell configuration is shown in Figure 3B, where the blue and red lines represent edge states. It can be seen that there are two points A and B corresponding to the same eigen-frequency (5.57 GHz). Figure 3C presents the electric field distribution of the points A and B, which shows the electromagnetic wave is well confined at the interface between

the topologically non-trivial and trivial lattices both for A and B. However, for the point A, the clockwise pseudo-spin mode is realized at the interface, and anticlockwise pseudo-spin mode is observed for the point B. The direction of the two pseudo-spin modes at the interface is opposite.

As shown in Figure 3B, there are two different pseudo-spin modes at the interface of topologically non-trivial and trivial lattices at the same frequency. As shown in Figure 3C, opposite spins of these modes can be verified. In general, each frequency of the topological band gap corresponds to two edge states, and the pseudo-spin directions of the two edge states are different. Electromagnetic waves with a certain pseudo-spin direction can only propagate in a fixed direction, which is consistent with the characteristics of the quantum Hall effect.

SHARP BEND WAVEGUIDES

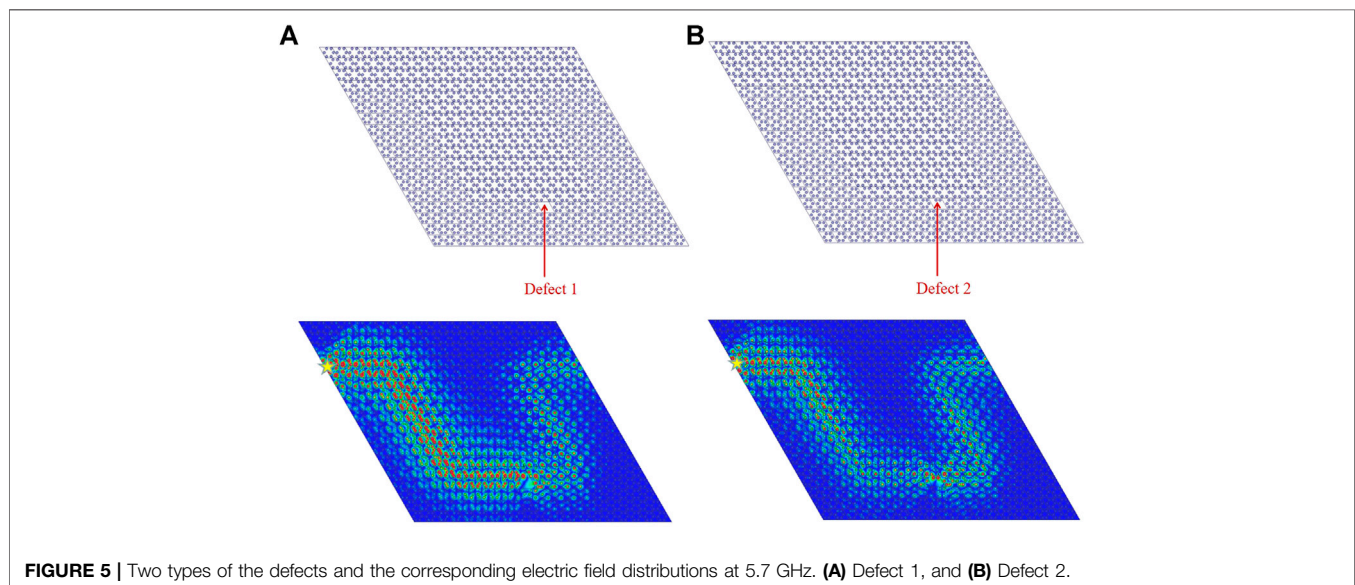
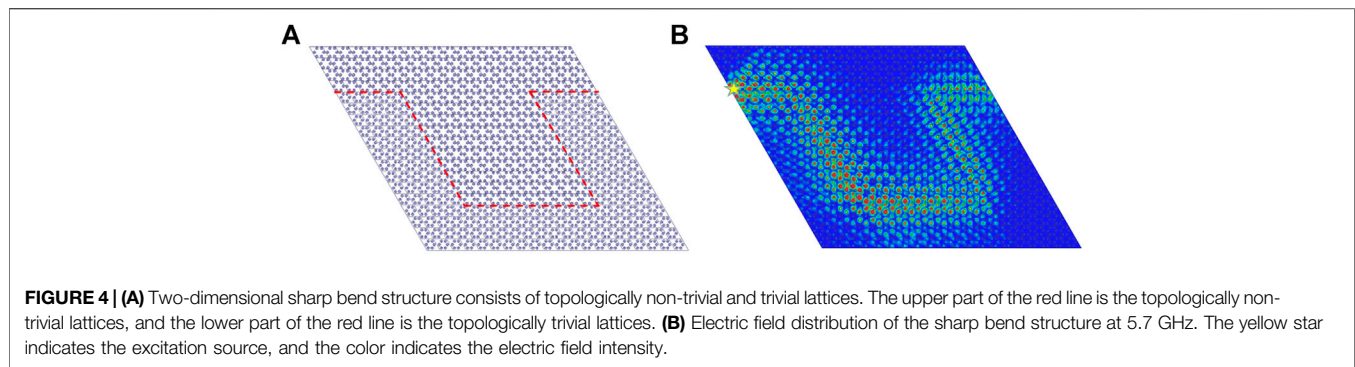
Since the proposed structure can support topological edge states, it is expected that new devices can be implemented by using this unique property. We construct a sharp bend interface by using two types of lattices ($R = 1.06a/3$ and $R = 0.91a/3$), which can operate as a directional waveguide. As shown in Figure 4A, we combine topologically non-trivial and topologically trivial lattices to form a two-dimensional sharp bend structure. The upper part of the red line is the topologically non-trivial lattices, and the lower part of the red line is the topologically trivial lattices. In this case, the interface of the two lattices has sharp angles.

In the simulation, the excitation source (denoted by a yellow star in Figure 4B) is set at the left side of the junction of the topologically non-trivial and trivial lattices. Radiation boundary conditions are introduced around the two-dimensional sharp bend structure. Simulation results show that the electromagnetic waves can propagate along the sharp bend interface in the frequency range of 5.54–5.8 GHz without obvious backscattering. Figure 4B presents the electric field distribution of the structure at 5.7 GHz, which shows electromagnetic waves can propagate along the sharp angles interface without back-scattering. The interface of the non-trivial transport operates like a waveguide.

In order to further verify the robustness of electromagnetic wave propagation along the sharp bend interface, as shown in Figure 5, two types of defects are introduced. For the defect 1 as presented in Figure 5A, six metal cylindrical resonators are removed from the topologically trivial lattices. The simulated electric field distribution shows there is no back-scattering and electromagnetic waves can transmit completely in this sharp bend interface. For the defect 2 as presented in Figure 5B, we remove the four resonators in the same topologically trivial lattices. As expected, the similar result is observed. Therefore, it can be seen that this non-trivial edge state transmission is robust.

CONCLUSION

To conclude, we present a design scheme for a topological material, consisting of six metal cylindrical resonators and a dielectric slab. The topological properties of the system are



studied numerically. Different topologically band gaps are achieved by via changing the geometric parameter R . It is demonstrated that the multi-cell configuration composed of two types of lattices with distinct topologies can generate topologically protected edge states. Moreover, the topologically protected edge states can be used to design a sharp bend waveguide, and it exhibits great robustness with immunity to imperfections. It can be expected that this edge state of backscattering suppression can have potential applications in optical transport and photonic integrated circuits.

DATA AVAILABILITY STATEMENT

The raw data supporting the conclusions of this article will be made available by the authors, without undue reservation.

REFERENCES

1. Qi XL, Zhang SC. Topological insulators and superconductors. *Rev. Mod. Phys* (2011) **83**:1057. doi:10.1103/revmodphys.83.1057

AUTHOR CONTRIBUTIONS

YL conceived the idea and supervised the project. LD and ML performed the numerical simulations. KS and XZ did the theoretical analysis. LD and YL co-wrote the manuscript.

ACKNOWLEDGMENTS

This work is supported by the National Natural Science Foundation of China (Grant Nos. 11874301, and 61601375), the Natural Science Basic Research Plan in Shaanxi Province of China (Grant No. 2020JM-094), and the Fundamental Research Funds for the Central Universities (Grant No. 310201911cx030).

- Hasan MZ, Kane CL. Colloquium: topological insulators. *Rev. Mod. Phys* (2010) **82**:3045. doi:10.1103/revmodphys.82.3045
- Wang Z, Chong Y, Joannopoulos JD, Soljačić M. Observation of unidirectional backscattering-immune topological electromagnetic states. *Nature* (2009) **461**(7265):772–5. doi:10.1038/nature08293

4. Khanikaev AB, Mousavi SH, Tse WK, Kargarian M, MacDonald AH, Shvets G. Photonic topological insulators. *Nature Mater* (2013) **12**:233–9. doi:10.1038/nmat3520
5. Liang GQ, Chong YD. Optical resonator analog of a two-dimensional topological insulator. *Phys Rev Lett* (2013) **110**:203904. doi:10.1103/physrevlett.110.203904
6. Hafezi M, Mittal S, Fan J, Migdall A, Taylor JM. Imaging topological edge states in silicon photonics. *Nature Photon* (2013) **7**:1001–5. doi:10.1038/nphoton.2013.274
7. He C, Sun XC, Liu XP, Lu MH, Chen Y, Feng L, et al. Photonic topological insulator with broken time-reversal symmetry. *Proc Natl Acad Sci USA* (2016) **113**(18):4924–8. doi:10.1073/pnas.1525502113
8. Chen BG, Upadhyaya N, Vitelli V. Nonlinear conduction via solitons in a topological mechanical insulator. *Proc Natl Acad Sci USA* (2014) **111**(36):13004–9. doi:10.1073/pnas.1405969111
9. Paulose J, Chen BG, Vitelli V. Topological modes bound to dislocations in mechanical metamaterials. *Nature Phys* (2015) **11**:153–6. doi:10.1038/nphys3185
10. Meussen AS, Paulose J, Vitelli J. Geared topological metamaterials with tunable mechanical stability. *Phys Rev X* (2016) **6**:041029. doi:10.1103/physrevx.6.041029
11. Nash LM, Kleckner D, Read A, Vitelli V, Turner AM, Irvine WTM. Topological mechanics of gyroscopic metamaterials. *Proc Natl Acad Sci USA* (2015) **112**(47):14495–500. doi:10.1073/pnas.1507413112
12. Süsstrunk R, Huber SD. Observation of phononic helical edge states in a mechanical topological insulator. *Science* (2015) **349**(6243):47–50. doi:10.1126/science.aab0239
13. Vila J, Pal RK, Ruzzene M. Observation of topological valley modes in an elastic hexagonal lattice. *Phys Rev B* (2017) **96**:134307. doi:10.1103/physrevb.96.134307
14. Xiao M, Ma G, Yang Z, Sheng P, Zhang ZQ, Chan CT. Geometric phase and band inversion in periodic acoustic systems. *Nature Phys* (2015) **11**:240–4. doi:10.1038/nphys3228
15. Khanikaev AB, Fleury R, Mousavi SH, Alu A. Topologically robust sound propagation in an angular-momentum-biased graphene-like resonator lattice. *Nat Commun* (2015) **6**:8260. doi:10.1038/ncomms9260
16. Mousavi SH, Khanikaev AB, Wang Z. Topologically protected elastic waves in phononic metamaterials. *Nat Commun* (2015) **6**:8682. doi:10.1038/ncomms9682
17. Fleury R, Khanikaev AB, Alu A. Floquet topological insulators for sound. *Nat Commun* (2016) **7**:11744. doi:10.1038/ncomms11744
18. He C, Ni X, Ge H, Sun XC, Chen YB, Lu MH, et al. Acoustic topological insulator and robust one-way sound transport. *Nature Phys* (2016) **12**:1124–9. doi:10.1038/nphys3867
19. Peng YG, Qin CZ, Zhao DG, Shen YX, Xu XY, Bao M, et al. Experimental demonstration of anomalous floquet topological insulator for sound. *Nat Commun* (2016) **7**:13368. doi:10.1038/ncomms13368
20. Liu TW, Sempertotti F. Tunable acoustic valley-hall edge states in reconfigurable phononic elastic waveguides. *Phys. Rev. Appl* (2018) **9**:014001. doi:10.1103/physrevapplied.9.014001
21. Geng ZG, Peng YG, Li PQ, Shen YX, Zhao DG, Zhu XF. Mirror-symmetry induced topological valley transport along programmable boundaries in a hexagonal sonic crystal. *J Phys Condens Matter* (2019) **31**(24):245403. doi:10.1088/1361-648x/ab0ffc
22. Fang C, Fu L. Rotation anomaly and topological crystalline insulators. arXiv:1709.01929 (2017)
23. Song ZD, Fang Z, Fang C. (d-2)-dimensional edge states of rotation symmetry protected topological states. *Phys Rev Lett* (2017) **119**:246402. doi:10.1103/physrevlett.119.246402
24. Schindler F, Cook AM, Vergniory MG, Wang Z, Parkin SSP, Bernevig BA, et al. Higher-order topological insulators. *Sci Adv* (2018) **4**:eaat0346. doi:10.1126/sciadv.aat0346
25. Liu YH, Guo QH, Liu HC, Liu CC, Song K, Yang K, et al. Circular-polarization-selective transmission induced by spin-orbit coupling in a helical tape waveguide. *Phys Rev Applied* (2018) **9**:054033. doi:10.1103/physrevapplied.9.054033
26. Yang B, Guo QH, Tremain B, Barr LE, Gao WL, Liu HC, et al. Direct observation of topological surface-state arcs in photonic metamaterials. *Nat Commun* (2017) **8**:97. doi:10.1038/s41467-017-00134-1.
27. Ma T, Khanikaev AB, Mousavi SH, Shvets G. Guiding electromagnetic waves around sharp corners: topologically protected photonic transport in metawaveguides. *Phys Rev Lett* (2015) **114**:127401. doi:10.1103/physrevlett.114.127401
28. Kane CL, Mele EJ. Quantum spin hall effect in graphene. *Phys Rev Lett* (2005) **95**:226801. doi:10.1103/physrevlett.95.226801
29. Bernevig BA, Hughes TL, Zhang SC. Quantum spin hall effect and topological phase transition in HgTe quantum wells. *Science* (2006) **314**(5806):1757–61. doi:10.1126/science.1133734
30. Wu LH, Hu X. Scheme for achieving a topological photonic crystal by using dielectric material. *Phys Rev Lett* (2015) **114**:223901. doi:10.1103/physrevlett.114.223901
31. Yang L, Yu K, Wu Y, Zhao R, Liu S. Topological spin-hall edge states of flexural wave in perforated metamaterial plates. *J Phys D Appl Phys* (2018) **51**(32):325302. doi:10.1088/1361-6463/aace49
32. Tzuhsuan M, Shvets G. Scattering-free edge states between heterogeneous photonic topological insulators. *Phys Rev B* (2017) **95**:165102. doi:10.1103/physrevb.95.165102
33. Huo SY, Chen JJ, Huang HB. Topologically protected edge states for out-of-plane and in-plane bulk elastic waves. *J Phys Condens Matter* (2018) **30**:145403. doi:10.1088/1361-648x/aab22a.
34. Xu L, Wang HX, Xu YD, Chen HY, Jiang JH. Accidental degeneracy in photonic bands and topological phase transitions in two-dimensional core-shell dielectric photonic crystals. *Opt Express* (2016) **24**:18059. doi:10.1364/oe.24.018059
35. Xie BY, Su GX, Wang HF, Wang HF, Su H, Shen XP, et al. Visualization of higher-order topological insulating phases in two-dimensional dielectric photonic crystals. *Phys Rev Lett* (2019) **122**:233903. doi:10.1103/physrevlett.122.233903
36. Lu L, Joannopoulos JD, Soljačić M. Topological photonics. *Nat Photon* (2014) **8**:821–29. doi:10.1038/nphoton.2014.248
37. Sun XC, He C, Liu XP, Lu MH, Zhu SN, Chen YF. Two-dimensional topological photonic systems. *Prog Quantum Electron* (2017) **55**:52–73. doi:10.1016/j.pquantelec.2017.07.004
38. Wu Y, Li C, Hu XY, Ao YT, Zhao YF, Gong QH. Applications of topological photonics in integrated photonic devices. *Adv Opt Mater* (2017) **5**(8):1700357. doi:10.1002/adom.201700357
39. Khanikaev AB, Shvets G. Two-dimensional topological photonics. *Nature Photon* (2017) **11**:763–73. doi:10.1038/s41566-017-0048-5
40. Ozawa T, Price HM, Amo A, Goldman N, Hafezi M, Lu L, et al. Topological photonics. *Rev Mod Phys* (2019) **91**:015006. doi:10.1103/RevModPhys.91.015006
41. Haldane FDM, Raghu S. Possible realization of directional optical waveguides in photonic crystals with broken time-reversal symmetry. *Phys Rev Lett* (2008) **100**:013904. doi:10.1103/physrevlett.100.013904
42. Zhang Z, Tian Y, Wang Y, Gao S, Cheng Y, Liu X, et al. Directional acoustic antennas based on valley-hall topological insulators. *Adv Mater* (2018) **30**(36):1803229. doi:10.1002/adma.201803229
43. Wei F, Liu CW, Li D, Wang CY, Zhang HR, Sun JR, et al. Broken mirror symmetry tuned topological transport in PbTe/SnTe heterostructures. *Phys Rev B* (2018) **98**:161301. doi:10.1103/physrevb.98.161301
44. Chaunsali R, Chen CW, Yang J. Subwavelength and directional control of flexural waves in zone-folding induced topological plates. *Phys Rev B* (2018) **97**:054307. doi:10.1103/physrevb.97.054307
45. Fukui T, Hatsugai Y, Suzuki H. Chern numbers in discretized Brillouin zone: Efficient method of computing (spin) Hall conductances. *J Phys Soc Jpn* (2005) **74**(6):1674–77. doi:10.1143/jpsj.74.1674

Conflict of Interest: The authors declare that the research was conducted in the absence of any commercial or financial relationships that could be construed as a potential conflict of interest.

Copyright © 2020 Du, Liu, Li, Ren, Song and Zhao. This is an open-access article distributed under the terms of the Creative Commons Attribution License (CC BY). The use, distribution or reproduction in other forums is permitted, provided the original author(s) and the copyright owner(s) are credited and that the original publication in this journal is cited, in accordance with accepted academic practice. No use, distribution or reproduction is permitted which does not comply with these terms.